Quantitative Proteomics Reveals Factors Regulating RNA Biology as Dynamic Targets of Stress-induced SUMOylation in *Arabidopsis**[S]

Marcus J. Miller‡, Mark Scalf§, Thérèse C. Rytz‡, Shane L. Hubler§, Lloyd M. Smith§, and Richard D. Vierstra‡¶

The stress-induced attachment of small ubiquitin-like modifier (SUMO) to a diverse collection of nuclear proteins regulating chromatin architecture, transcription, and RNA biology has been implicated in protecting plants and animals against numerous environmental challenges. In order to better understand stress-induced SUMOylation, we combined stringent purification of SUMO conjugates with isobaric tag for relative and absolute quantification mass spectrometry and an advanced method to adjust for sample-to-sample variation so as to study quantitatively the SUMOylation dynamics of intact *Arabidopsis* seedlings subjected to stress. Inspection of 172 SUMO substrates during and after heat shock (37 °C) revealed that stress mostly increases the abundance of existing conjugates, as opposed to modifying new targets. Some of the most robustly up-regulated targets participate in RNA processing and turnover and RNA-directed DNA modification, thus implicating SUMO as a regulator of the transcriptome during stress. Many of these targets were also strongly SUMOylated during ethanol and oxidative stress, suggesting that their modification is crucial for general stress tolerance. Collectively, our quantitative data emphasize the importance of SUMO to RNA-related processes protecting plants from adverse environments. ***Molecular & Cellular Proteomics 12: 10.1074/mcp.M112.025056, 449–463, 2013.***

The ability of cellular organisms to cope with environmental challenges requires the detection and immediate initiation of defense responses designed to mitigate the damage inflicted and enhance the organism's ability to tolerate future insults. For sessile organisms such as plants, robust stress responses are fundamental to their survival in a wide range of adverse environments (1, 2). Genetic and biochemical studies have identified a plethora of input pathways and output responses for stress protection in both prokaryotes and eukaryotes. Universally important is the synthesis of heat shock proteins that minimize protein aggregation and stimulate protein refolding through intrinsic chaperone activities (3).

The stress-induced modification of intracellular proteins by small ubiquitin-like modifier (SUMO)[1] has recently emerged as an additional line of defense in eukaryotes (4–6). Attachment of the ~100-amino-acid SUMO protein is driven by an ATP-dependent, three-step enzyme cascade, which in *Arabidopsis thaliana* involves the E1 heterodimer (SAE2 together with either of two SAE1 isoforms), a single E2 SCE1, and at least two E3s (SAP, MIZ1 (SIZ1), and MMS21/HYP2) (7–11). The end result is the isopeptide linkage of one or more SUMO moieties to accessible target lysine(s). Most commonly, a consensus ΨKxE SUMO-binding motif is modified, where Ψ represents a bulky hydrophobic residue (12, 13). In some cases, the bound SUMOs themselves are also substrates, which results in poly-SUMO chains decorating the target (14, 15). Once generated, SUMO conjugates can be disassembled by a family of deSUMOylating proteases that specifically cleave these isopeptide bonds, thus allowing SUMO to act reversibly (*e.g.* Refs. 7, 16–18).

Important with regard to stress protection are observations that the abundance of SUMO conjugates rises dramatically and reversibly when yeast, animals, and plants are exposed to numerous environmental stresses (7, 19, 20). For example, a substantial increase in conjugates assembled with the SUMO1 and SUMO2 isoforms can be detected within minutes after treating *Arabidopsis* seedlings to a relatively mild heat shock (37 °C), and this can be subsequently reversed upon a return to non-stress temperatures (7). Genetic studies have demonstrated that SUMOylation is both essential for normal cellular functions and critical for stress protection (8, 21–23). For *Arabidopsis* in particular, mutants missing the SIZ1 E3 that drives most stress-induced SUMOylation (8) are hyper-

From the ‡Department of Genetics, 425-G Henry Mall, University of Wisconsin-Madison, Madison, Wisconsin 53706; §Department of Chemistry, 1101 University Ave., University of Wisconsin-Madison, Madison, Wisconsin 53706

Received October 19, 2012, and in revised form, November 28, 2012

Published, MCP Papers in Press, November 29, 2012, DOI 10.1074/mcp.M112.025056

[1] The abbreviations used are: FDR, false discovery rate; HSF, heat shock transcription factor; iTRAQ, isobaric tag for relative and absolute quantitation; Ni-NTA, nickel–nitrilotriacetic acid; PSM, peptide spectrum match; SILAC, stable isotope labeling of amino acids in cell culture; SIZ1, SAP and MIZ1 SUMO E3 ligase; SUMO, small ubiquitin-like modifier; Ub, ubiquitin.

sensitive to various stresses, including heat, cold, drought, flooding, high salt, and phosphate and nitrate starvation (9, 17, 24–28); are hyposensitive to pathogens (29, 30); and have altered signaling by the stress hormones abscisic acid and salicylic acid (29–33). Similar connections have been observed in animals, including roles in anaerobic tolerance (34, 35) and genotoxic stress (36). Numerous plant and animal pathogens also have been shown to synthesize factors that promote infection by interfering with host SUMOylation (37, 38).

Studies on individual targets have implicated SUMO in a variety of essential processes relevant to signal transduction, the cell cycle, nuclear/cytoplasmic partitioning, ribosome biogenesis, DNA repair, and ubiquitin (Ub)-mediated protein breakdown (4–6). For many targets, only a small proportion needs to be SUMOylated to achieve maximal effect; this "SUMO enigma" implies that SUMO addition does not activate/inactivate its targets *per se* but might drive cycles critical for their action (*e.g.* assembly/disassembly of transcription complexes, nuclear/cytoplasmic shuttling, or protein degradation) (4). Some of these activities are mediated through SUMO-interacting motifs (SIMs) present within binding partners (39, 40). More recent proteomic studies on stress-induced SUMOylation found a strong emphasis on nuclear targets, with their collective functions implying that SUMO participates in stress protection by regulating chromatin architecture, the transcriptome, and protein quality control (15, 20, 41–44). In *Arabidopsis*, the list of over 350 SUMO1/2 targets includes histones H1 and H2B, complexes involved in DNA and histone modifications, various transcription factors and co-activators/co-repressors, RNA-binding proteins, and subunits of the nuclear pore complex, as well as various components of the SUMO pathway (41). Similar classes of regulators have been identified in interactome studies using the *Arabidopsis* SCE1 E2 and the ESD4 deSUMOylating protease as baits (45).

Full appreciation of stress-induced SUMOylation clearly requires identification of the most robustly affected targets and the ways in which their SUMOylation status changes during and after stress. Such global quantification has recently become possible through advances in proteomic technologies, including the stable isotope labeling of amino acids in cell culture (SILAC) mass spectrometry (MS) approach (20, 42). Although SILAC-MS has advantages for cell cultures that permit facile protein labeling via the addition of isotopically tagged amino acids to the growth medium, its use remains challenging for intact organisms generally, and for plants in particular, which naturally synthesize the full complement of amino acids (46, 47). To overcome these difficulties, we combined a stringent purification method for SUMO conjugates with the isobaric tag for relative and absolute quantification (iTRAQ) method (48, 49) and an advanced SUMO-based normalization strategy to accurately measure the changes in SUMOylation state for individual substrates in intact *Arabidopsis* plants under stress. By tracking SUMO1/2 substrates before, during, and after a mild heat shock (37 °C), or following oxidative and ethanol stress, we identified a catalogue of substrates that are robustly SUMOylated after environmental challenges. Included are proteins critical for RNA processing, stability, and export; proteins regulating RNA-directed DNA modifications and heterochromatin condensation; transcription factors that regulate the heat shock response; and a to-be-defined collection that becomes both SUMOylated and ubiquitylated. Taken together, our data point to the SUMO-mediated control of numerous nuclear processes, especially those related to RNA biogenesis and use, as vital for protecting plants during stress and providing subsequent acquired tolerance.

EXPERIMENTAL PROCEDURES

Plant Materials and Quantitative Immunoblot Analysis—All experiments were conducted with the *Arabidopsis thaliana* Columbia-0 ecotype grown at 24 °C in liquid culture under continuous light (7, 41). Heat, ethanol, and oxidative stress involved exposing the cultures to 37 °C, 10% ethanol, or 50 mM H_2O_2 for the indicated times. Total protein was extracted from whole seedlings by pulverizing frozen tissue in 2 ml/g fresh weight of 20% glycerol, 4% SDS, 10% 2-mercaptoethanol, and 125 mM Tris-HCl (pH 6.8). Immunoblots were conducted with anti-SUMO1 and anti-PBA1 antibodies as described elsewhere (7). Quantitative immunoblotting was performed with the IRDye 800CW secondary antibody, and this was followed by detection with the Odyssey imaging system (LI-COR Biosciences, Lincoln, NE). Rabbit anti-SIZ1 antibodies were generated against a 6His-tagged fragment (residues 59–537) expressed recombinantly and purified from the inclusion body fraction using the BugBuster Master Mix (EMD Millipore, Darmstadt, Germany), and this was followed by nickel–nitrilotriacetic acid (Ni-NTA) chromatography (Qiagen, Valencia, CA). The antibodies were purified via binding to the SIZ1 fragment adhered to PVDF membranes and subsequent elution with 200 mM glycine (pH 2.5). Proteins modified with both Ub and SUMO were enriched through Ni-NTA chromatography from a transgenic line expressing a hexameric repeat of 6His-Ub (50). A pH 6.3 wash step was included to help remove nonspecific binding proteins.

Protein Purification and iTRAQ Labeling—SUMOylated proteins were enriched from 35 g of *6His-SUMO1-H89R sumo1–1 sumo2–1* seedling via the three-step affinity method (described previously), which involves sequential Ni-NTA, anti-SUMO1 affinity, and Ni-NTA chromatographic steps (41), and digested in solution with sequencing-grade trypsin (Promega, Madison, WI). Prior to purification, each sample was spiked with 5 μg of 6His-SUMO2 synthesized recombinantly and purified via Ni-NTA affinity chromatography (7). All subsequent steps were completed using Protein LoBind tubes (Eppendorf, Hamburg, Germany). Tryptic peptides were acidified with 10% trifluoroacetic acid to a final concentration of 0.5%, desalted using C_{18} sold-phase extraction (Varion Omix tips, 70 μg capacity), and dried completely *in vacuo*. Peptides were resuspended in 33 μl of the dissolution buffer included in the 4-Plex iTRAQ kit (without SDS) and conjugated with one of the four isobaric tags per the manufacturer's recommendations (AB Sciex, Framingham, MA). The tag order was reversed among the biological replicates to avoid potential discrimination. The labeled samples were vacuum dried to ~50 μl (half of the original volume), mixed with 400 μl water, and pooled. The mixed samples were acidified, desalted via C_{18} sold-phase extraction, dried *in vacuo*, and resuspended in 10 μl of 95% water, 5% acetonitrile, and 0.1% formic acid.

Liquid Chromatography–Electrospray Ionization–MS/MS Analysis—The iTRAQ-labeled pools were fractionated via reversed-phase liquid chromatography (LC) (nanoAcquity, Waters, Milford, MA) and injected

online into an electrospray ionization (ESI) Fourier transform (FT)/ion-trap mass spectrometer (LTQ Orbitrap Velos, Thermo Fisher Scientific, Waltham, MA). LC separation involved a 50 μm $\times$ 365 μm fused silica capillary micro-column packed with 15 cm of 5-μm-diameter C18 beads (Western Analytical Products, Wildomar, CA) preceded by a 5-cm trap column (75 μm $\times$ 365 μm, 5-μm-diameter C18 beads). Peptides were injected over 20 min at a flow rate of 1 μl/min and eluted over 180 min at a flow rate of 200 nl/min with a gradient of 5% to 50% acetonitrile in 0.1% formic acid. Full-mass scans were performed in the FT orbitrap at 300–1500 *m/z* at a resolution of 60,000, and this was followed by ten MS/MS high-energy collisional dissociation (HCD) scans of the ten highest intensity parent ions at 45% relative collision energy and 7500 resolution, with a mass range starting at 100 *m/z*. Dynamic exclusion was enabled with a repeat count of two over a duration of 30 s and an exclusion window of 90 s.

Database Searches, iTRAQ Quantification, and Bioinformatic Analysis—The acquired MS and MS/MS spectra were searched against the *A. thaliana* ecotype Col-0 protein database (IPI database version 3.61, containing 37,185 entries) using the software package Proteome Discover 1.3. All raw spectra are available in the Peptide Atlas database. Spectra to search were selected using the Spectrum Selector module, with the requirements of a mass between 400 and 5500 amu and a signal-to-noise cut-off of greater than 3, and were searched using SEQUEST version 1.2 (Thermo Fisher Scientific). Masses for both precursor and fragment ions were treated as monoisotopic. Oxidized methionine (+15.995 Da), carbamidomethylated cysteines (+57.021 Da), and iTRAQ-labeled tyrosine (+144.102 Da) were included as variable modifications. iTRAQ-labeled (+144.102 Da) N-terminal amino acids and lysine (in case of missed cleavages) were included as static modifications. The database search also allowed for up to two missed trypsin cleavages. Ion masses were matched with a mass tolerance of 10 ppm for precursor masses and 0.1 Da/mz for HCD fragments. The data were filtered using a 5% peptide false discovery rate (FDR) (51). To search for possible SUMO and Ub footprints (QTGG or GG isopeptide linked to K, respectively (41, 50)), the database search was modified to include (i) a cyclized N-terminal glutamine (mass shift of 326.12 Da) for SUMO footprints, (ii) a non-cyclized version of the SUMO footprint with an N-terminal iTRAQ tag (total mass shift of 487.25 Da), and (iii) the Ub footprint (GG) with an N-terminal iTRAQ tag (mass shift of 258.25 Da). These data were filtered using a 1% peptide FDR.

iTRAQ quantification was determined using the Proteome Discoverer 1.2 software (Thermo Fisher Scientific). Each biological replicate combined the data from three or four technical replicates. Only those proteins detected by at least two unique peptides in each biological replicate were included in the final analysis. The iTRAQ values calculated for each protein were derived from all protein-specific peptide spectrum matches (PSMs) based on peak areas within a mass precision window of 20 ppm and a cutoff intensity of 3-fold over background, and they were expressed as a ratio relative to the values calculated at $t = 0$. The raw quantitative numbers were adjusted using the isotopic impurity values provided by the manufacturer for each isobaric tag (114: $-1 = 0.58\%$, $0 = 94.52\%$, and $+1 = 4.9\%$; 115, $-1 = 0.59\%$, $0 = 94.77\%$, and $+1 = 4.64\%$; 116, $-1 = 1.38\%$, $0 = 95.84\%$, and $+1 = 2.78\%$; and 117, $-1 = 2.13\%$, $0 = 95.18\%$, and $+1 = 2.69\%$) (52). All iTRAQ data, including rare situations in which one or more of the iTRAQ reporter peaks were not identified (see supplemental Dataset S2), were included in the final calculations of fold change for individual peptides. Replacing absent peaks with a minimal background intensity value did not change the catalogue of targets, nor did it appreciably affect their quantification (data not shown).

To validate the iTRAQ quantification, samples were generated by mixing and digesting equal volumes of purified SUMO conjugates obtained at each of four heat stress time points ($t = 0$, 0.5, 1.5, and 4 h) together in solution with trypsin, and then aliquots were separately labeled with each of four iTRAQ reagents. The resulting reactions were pooled at varying ratios (1:8:2 and labeled with iTRAQ reagents 114:115:117 (Ratio 1), and 1:16:4:1.5 and labeled with iTRAQ reagents 114:115:116:117 (Ratio 2)) and then subjected to MS quantification as described above, with the exceptions that the contaminants were not subtracted from the list and the peptides were not normalized to the internal 6His-SUMO2 standard. iTRAQ-MS analysis of spiked 6His-SUMO2 and 80 and 70 other *Arabidopsis* proteins enriched during SUMO conjugate purification for Ratios 1 and 2, respectively, were used to determine the mean fold-change values and standard deviation (S.D.) for each dilution. A parallel MS analysis was performed with samples purified from wild-type seedlings exposed to a 30-min 37 °C heat shock followed by a 30-min recovery. This catalogue of 59 contaminants (supplemental Dataset S1) was subtracted from those obtained using the *6His-SUMO1-H89R sumo1–1 sumo2–1* line.

We analyzed the quantitative iTRAQ MS data using Excel workbooks developed in house to reconstitute channel measurements and compute *p* values, FDR, and global mean changes between the different conditions and/or time points. Because the raw data were expressed as channel ratios, we reconstituted any missing channel ratio by replacing it with 1 and then renormalizing all the channels by the geometric mean across conditions (performed on each protein separately). This process theoretically reduced the nuisance noise by 40% and allowed us to relate biological replicates and perform statistical analyses (*e.g. t* tests) on channel combinations. *p* values were calculated using a two-tailed *t* test assuming equal variance for the two compared groups. For the heat-stress time series, we compared the first time point ($t = 0$) to each of the other time points individually. For the multi-stress analysis, we compared each condition to all other conditions including non-stressed samples, which provided us with a list of proteins that changed significantly for each condition. FDRs were determined one comparison at a time (*e.g.* $t = 0$ *versus* $t = 0.5$ h separately from $t = 0$ *versus* $t = 1.5$ h) by estimating the total number of non-changing proteins, estimating the number of false positives for each *p* value, computing a raw FDR score, and then computing a final FDR. The number of non-changing proteins was estimated by counting the number of proteins with a *p* value greater than 0.5 and multiplying the result by 2. This result was multiplied by a given *p* value to estimate how many false positives would be expected if that *p* value were used as a criterion cut-off. The raw FDR divided this product by the actual number of proteins with that *p* value or less. Finally, we created the final FDR by converting the raw FDR to a non-decreasing function of *p*.

Functional enrichments of SUMOylated proteins were determined using the gene ontogeny (GO) Singular Enrichment analysis tool from AgriGO with the *Arabidopsis* gene models (TAIR9) background reference, setting a *p* value cutoff of <0.001. Possible SUMO-binding sites were identified using the high-probability threshold in SUMOsp 2.0 (53). Heat maps were generated using Java TreeView.

RESULTS

Quantifying Global Changes in SUMOylation during Heat Stress—Prior non-quantitative studies documented the changes in SUMOylation during and after a heat stress of *Arabidopsis* seedlings and revealed a dynamic time course in which heat (37 °C) rapidly induces the accumulation of SUMO1/2 conjugates, and this increase is followed by a slower decline after the seedlings are returned to their normal growth temperature (24 °C) (7, 8) (Fig. 1*A*). In order to more

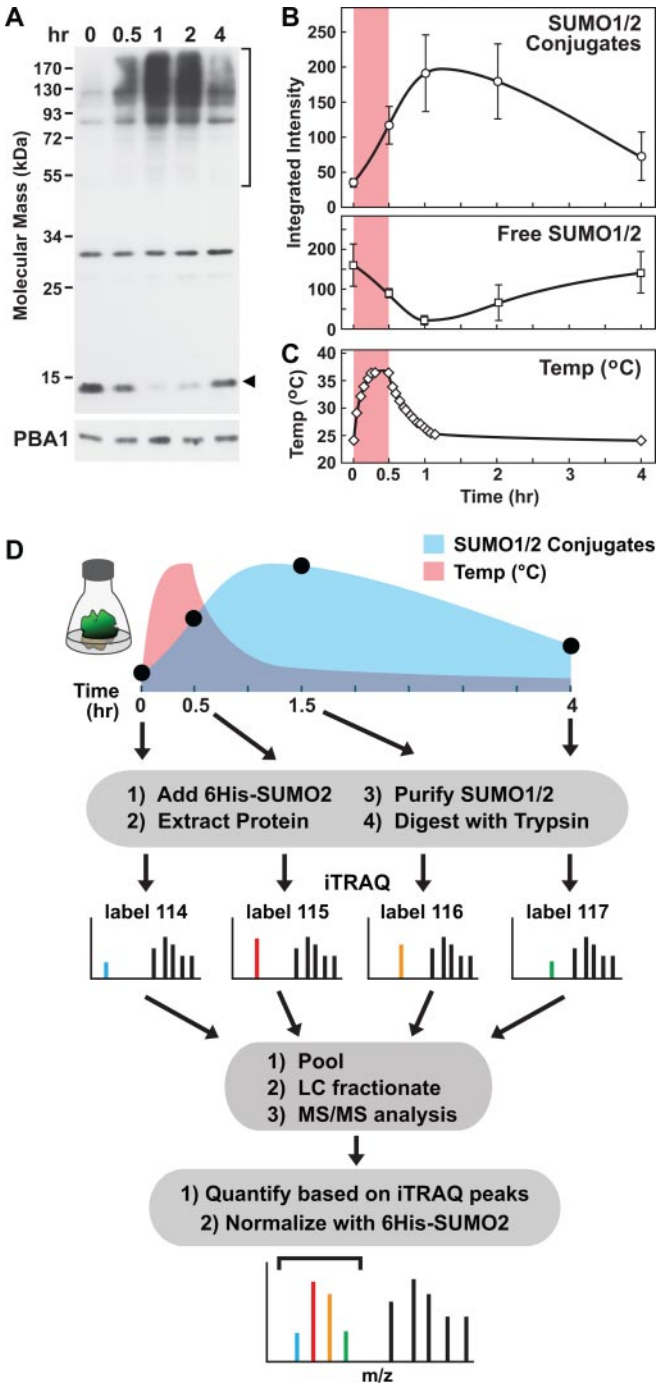

FIG. 1. **SUMO1/2 conjugates rapidly accumulate in *Arabidopsis* seedlings during heat stress.** *A*, immunoblot analysis of SUMO1/2 conjugates from wild-type plants before and immediately after a 30-min heat shock at 37 °C followed by recovery at 24 °C. An anti-PBA1 immunoblot is included to confirm equal protein loads. The arrowhead and bracket locate free and conjugated SUMO1/2, respectively. *B*, measurement of free SUMO1/2 and their conjugates before and after the heat shock in (*A*) via quantitative immunoblot analysis. Each point represents the average of three biological replicates (±1 S.D.). *C*, temperature of the cultures during the heat shock time course. The shaded areas in (*B*) and (*C*) highlight when the cultures were exposed to 37 °C. *D*, flow chart describing the protocol used to quantify SUMO1/2 conjugates by means of iTRAQ MS along with the method to adjust for sample-to-sample variation by spiking with recombinant 6His-SUMO2.

accurately describe these kinetics, we employed a linear fluorescence-based immunodetection system to measure the pools of free and conjugated SUMO1/2 (Figs. 1*B*, 1*C*). The antibodies used recognize SUMO1 and SUMO2 well, but not the other SUMO isoforms expressed in *Arabidopsis* (7). This analysis showed that SUMO1/2 conjugate levels rise rapidly upon a 30-min 24 °C to 37 °C up-shift and continue to rise during the early recovery phase as the temperature returns to normal, with the peak of SUMO1/2 conjugates representing a ~6-fold (±1.8 S.D., $n = 3$) increase. A parallel drop and reappearance of free SUMO1/2 mirrored this rise, with the trough representing a ~8-fold (±2.0 S.D., $n = 3$) decline (Figs. 1*B*, 1*C*). After a 3.5-h incubation at the non-stress temperature, the levels of SUMO1/2 conjugates and free SUMO1/2 almost returned to their pre-stress levels, illustrating the reversibility of the response.

Development of a Quantitative Proteomic Strategy to Monitor Changes in SUMOylation—Prior proteomic studies revealed that the high molecular mass collection of SUMO1/2 conjugates in *Arabidopsis* seedlings before and after heat shock includes over 350 nuclear-enriched substrates, with evidence that some are strongly SUMOylated by heat stress, whereas others are only weakly affected or even deSUMOylated (41). To better appreciate the molecular consequences of this stress-induced SUMOylation, we developed a quantitative proteomic method amenable to intact plants that would help identify the most robustly regulated substrates (up or down). In order to avoid the inherent difficulties of SILAC MS (46, 47), we instead employed the iTRAQ labeling system to measure the relative abundance of specific peptides via tandem MS (48, 49). This approach was combined with a three-step protocol to purify SUMO1 conjugates under stringent denaturing conditions (6 M guanidine-HCl and 8 M urea) from transgenic plants that were engineered to replace the two essential SUMO isoforms involved in stress-induced SUMOylation (SUMO1 and SUMO2 (8)) with a 6His-SUMO1-H89R variant designed for faithful genetic rescue, efficient purification, and better mapping of SUMO attachment sites (41).

Using the workflow illustrated in Fig. 1*D*, 7-day-old *6His-SUMO1-H89R sumo1–1 sumo2–1* seedlings grown in liquid culture were collected before and after a 30-min up-shift from 24 °C to 37 °C ($t = 0$, 0.5, 1.5, and 4 h), and free SUMO1/2 and SUMO1 conjugates were then affinity purified. Comparisons utilizing protein staining and immunoblot analysis with anti-SUMO1 antibodies confirmed that the final preparations were highly enriched in SUMO1 conjugates and that the levels of these conjugates reflected well their abundance in the plants during the heat-stress time course (supplemental Fig. S1*A*). Trypsinized peptides from each time point were labeled

separately with one of the four unique iTRAQ isobaric tags, combined, and then analyzed via MS/MS in the HCD mode. As designed (49), each of the iTRAQ-labeled peptides would have the same parent mass but, upon MS/MS fragmentation, would generate diagnostic ion quadruplets at 114, 115, 116, and 117 *m/z* (supplemental Fig. S2*D*); the ratio of these ion signals reflects the relative abundance of the peptide and, thus, the parent protein at each time point.

The technical challenges associated with accurate iTRAQ quantification typically involve variations in isobaric tag labeling efficiency, background interference during precursor ion selection for complex samples, and the inconsistent preparation of each time point sample before mixing, which is especially problematic here given the three column steps (sequential Ni-NTA, anti-SUMO1/2 affinity, and Ni-NTA chromatography) that would be used to purify SUMO1 conjugates (52, 54). To help adjust for such variations, we developed an innovative normalization strategy that exploits 6His-SUMO2 as an internal control (Fig. 1*D*). Its use was made possible by (i) the absence of SUMO2 in *6His-SUMO1-H89R sumo1–1 sumo2–1* plants; (ii) its strong recognition by anti-SUMO1 antibodies in addition to binding Ni-NTA (supplemental Fig. S2*B*), which enabled effective co-purification with 6His-SUMO1 and its conjugates generated *in planta*; and (iii) the fact that despite SUMO2 being 93% identical to SUMO1 at the amino acid sequence level, its trypsinization generates four unique peptides unequivocally identifiable via MS/MS that could be used for iTRAQ quantification (supplemental Figs. S2*A*, S2*C*, and S2*D*). Our strategy was to add an equal amount of purified recombinant 6His-SUMO2 to each crude extract before purification, iTRAQ-MS quantify the four unique 6His-SUMO2 peptides recovered in the final mixed sample, and then use the combined averaged iTRAQ values from these 6His-SUMO2 peptides to normalize the relative fold changes of all SUMO substrates among the time points. Prior measurements indicated that the amount of 6His-SUMO2 added to each sample (5 μg) represented approximately one-tenth of the total amount of 6His-SUMO1 (both free and conjugated) extracted from 35 g of *6His-SUMO1-H89R sumo1–1 sumo2–1* plants.

Importantly, by using consistent purification and labeling techniques, we obtained relatively uniform measurements of 6His-SUMO2 in our time course samples that deviated by at most 1.68-fold (supplemental Figs. S2*C*, S2*D*). Our best recoveries of 6His-SUMO2 typically coincided with the highest levels of SUMO1 conjugates and the lowest levels of free 6His-SUMO1-H89R (t = 1.5 h), suggesting that the immunoaffinity recovery of free 6His-SUMO2 was dampened modestly by the greater competitive binding of free SUMO1 relative to SUMO1 conjugates. Despite their overall consistency, subsequent use of the 6His-SUMO2 correction values ensured that no major biases were introduced during the purification and labeling steps, improved statistical comparisons among technical and biological replicates, and, if anything, made our corrected values for the relative rise in SUMO1/2 conjugates during heat stress slightly more conservative than the measured values.

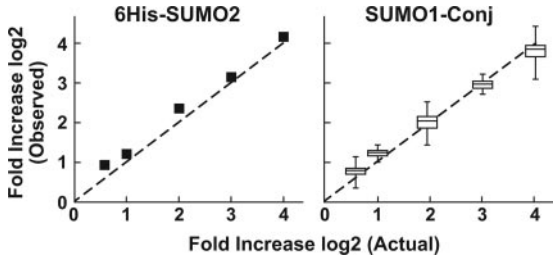

FIG. 2. **Accuracy of iTRAQ MS in quantifying the abundance of *Arabidopsis* SUMO conjugates.** A SUMO conjugate preparation spiked with 6His-SUMO2 was generated by pooling samples purified from all four time points during a 30-min heat shock time course (t = 0, 0.5, 1.5, and 4 h) (see Fig. 1*D*) and then was labeled separately with each of the four iTRAQ reporters (114, 115, 116, and 117) and mixed at various ratios from 1- to 16-fold. The samples then underwent iTRAQ-MS analysis. The left and right panels show the respective quantification of 6His-SUMO2 and a collection of purified *Arabidopsis* proteins (n = 70 and 80 for replicate samples). The experimental data for the heterogeneous collection of proteins are presented as box plots, with the boxes indicating the second and third quartiles, respectively, and the error bars encompassing 2 S.D. above and below the mean. The dashed line in both panels reflects the expected fold increases for the mixed samples.

To help demonstrate that our quantitative strategy also accurately described the fold changes for individual SUMO conjugates during and after heat shock, we generated a pooled sample that combined equivalent volumes from each time point (t = 0, 0.5, 1.5, and 4 h). Aliquots of this sample were individually labeled with each of the 114, 115, 116, and 117 iTRAQ reagents and then mixed at varying ratios up to 16-fold. The amounts of spiked 6His-SUMO2 and the heterogeneous collection of purified *Arabidopsis* proteins were then measured via MS/MS based on the iTRAQ reporter quadruplets for all available daughter peptides. As shown in Fig. 2, the quantified amounts of recombinant 6His-SUMO2 and the collection of endogenous proteins (70 and 80 from two replicates) closely adhered to their actual amounts and gave strikingly consistent mean values for changes ranging from 1.5- to 16-fold (S.D. $\pm$ 0.2, 0.2, 0.7, 0.7, and 2.6, respectively).

In addition to the stringent purification protocol, multiple steps were taken to reduce the number of false positives in the final dataset and improve the quantification accuracy. First, only those proteins quantified by two or more high-confidence SEQUEST-scored peptides in each of two biological replicates were included in the final dataset (Fig. 3*A*). Second, any proteins also identified in a mock purification using wild-type seedlings collected during the early recovery phase after heat shock (t = 1.5 h), when endogenous SUMO1 conjugate levels are generally the highest, were considered as nonspecific contaminants and were culled from the final dataset (supplemental Dataset S1). As evidenced by the presence of the known SUMO substrate TIC (detected by a SUMO

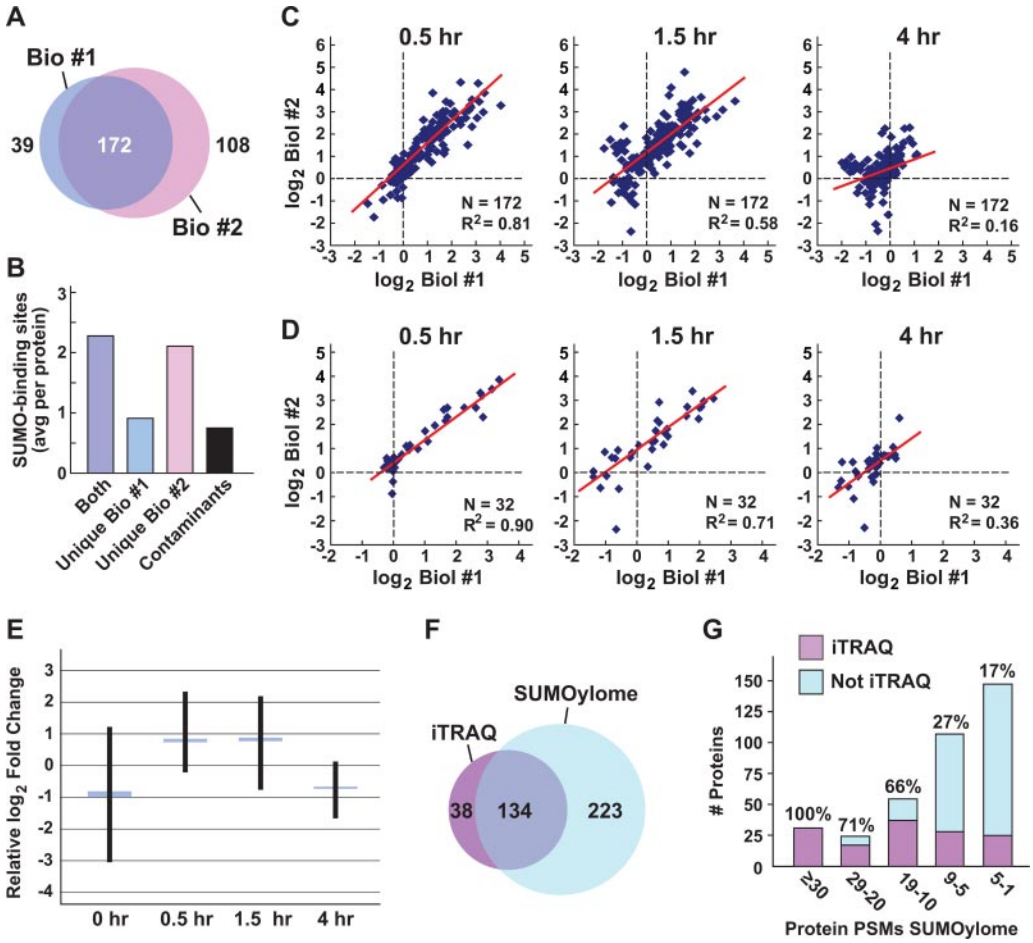

FIG. 3. **iTRAQ MS reproducibly quantified the relative SUMOylation state for 172 *Arabidopsis* targets.** The conjugates were purified from *6His-SUMO1-H89R sumo1–1 sumo2–1* seedlings before and immediately after a 30-min heat shock at 37 °C followed by recovery at 24 °C. *A*, Venn diagram showing the overlap of quantified proteins identified from two biological replicates. *B*, identified SUMO1/2 targets are enriched for the consensus ΨKxE SUMO binding site. The average number of high-probability sites per protein was compared for proteins identified in both biological replicates, unique to each replicate, or found in contaminants purified from wild-type plants. *C*, *D*, reproducibility of iTRAQ quantification for the SUMOylated proteins detected in both biological replicates. The $\log_2$ fold change of each target at $t = 0.5$, 1.5, and 4 h was compared with that at $t = 0$. The lines of best-fit linear regression (red) and the corresponding R^2 values are included. (*C*) and (*D*) represent the analysis of 172 and 32 targets that met the PSM cutoffs of ≥2 and ≥20, respectively. *E*, Whisker plots showing the distribution of fold change values for each time point. Blue boxes indicate 95% confidence intervals of the means, and lines encompass the range from maximum to minimum values. *F*, Venn diagram illustrating the overlap between SUMO substrates quantified in this study as compared with the more complete *Arabidopsis* catalogue detected via non-quantitative MS (41). *G*, comparison of SUMOylated proteins detected here via iTRAQ MS *versus* those detected via non-quantitative MS based on the number of PSMs for each protein. Purple shades highlight the number of proteins in each PSM bin that were among the 172 proteins quantified in our current study. The percent overlap between the two datasets is stated above each bar. Data and statistical analysis for all targets can be found in supplemental Dataset S2.

footprint (41)) in the mock dataset, it is possible that some SUMOylated proteins were eliminated as contaminants.

Validation of Our Quantitative Proteomic Dataset—Using the above quantitative iTRAQ-MS protocol, normalization strategy, and identification criteria, we successfully determined the relative fold change in SUMOylation over a heat-stress time course for 172 unique substrates; see supplemental Dataset S2 for the complete list and supplemental Fig. S4 for representative MS/MS spectra. The mean fold change for heat-stress time points $t = 0.5$ and 1.5 h was significantly greater than that for contaminant proteins or for SUMOylated proteins isolated before or after the stress ($t = 0$ and 4 h (Fig. 3*E*)). In fact, the change at peak accumulation calculated for the sum of SUMOylated targets (~3.8-fold up) was close to that measured by immunoblotting (Fig. 1*B*). Contributing to this global increase, 112 out of 172 individual targets were found to undergo a statistically significant ($p < 0.05$, FDR < 0.07) change in SUMOylation during and soon after heat stress ($t = 0.5$ or 1.5 h) (supplemental Dataset S2). Taken together, these observations support a scenario in which the SUMOylation status of most targets increases during stress.

The validity of the iTRAQ-MS dataset was supported by (i), the strong overlap (82%) between two independent biological replicates (Fig. 3*A*), (ii) significant enrichment for proteins

bearing the consensus ΨKxE SUMO-binding motif (2.29 sites per protein ($n = 172$) *versus* 0.75 predicted for the contaminants ($n = 59$) (Fig. 3*B*), and (iii) strong overlap of this dataset (78%) with that obtained previously for *Arabidopsis* seedlings via non-quantitative MS (41) (Fig. 3*F*). Furthermore, the proteins identified here by iTRAQ MS were typically the most common SUMO substrates identified non-quantitatively as determined by PSM counts (Fig. 3*G*), indicating that our list of 172 targets likely provides excellent coverage of the major SUMOylated proteins in *Arabidopsis*. We note that the 108 proteins unique to biological replicate 2 (supplemental Dataset S2) were also significantly enriched for the ΨKxE motif (2.12 sites per protein), suggesting that some of these proteins are also *bona fide* SUMO substrates (Fig.3*B*).

To help validate the quantitative values assigned to each target, we compared the relative fold change of all 172 targets before and after the 0.5-h heat stress for the two biological replicates. As can be seen in Fig. 3*C*, significant correlations were observed for the 0.5- and 1.5-h values ($R^2 = 0.81$ and 0.58, respectively), with the correlation becoming weak as expected after 4 h ($R^2 = 0.16$) as the profile of SUMO conjugates returned to nearly pre-stress values. Some of the variance at 0.5 and 1.5 h could be explained by technical variability inherent in the iTRAQ-MS analysis. In support, when the same iTRAQ-labeled sample was subjected to two independent MS runs, the calculated fold change values were imperfectly correlated, with R^2 values of 0.88, 0.86, and 0.74 for the $t = 0.5$, 1.5, and 4 h time points, respectively. We predicted that the iTRAQ-MS quantification for individual targets would become more precise if iTRAQ data from more PSMs were included in the final calculations. This appears to be the case, as tighter correlations among technical and biological repeats were evident as the minimum PSM cutoffs were increased from 2 to 20 for the biological replicates and from 2 to 7 for the technical replicates (Figs. 3*C* and 3*D*, and data not shown). Consequently, we recommend incorporating information on PSM counts when judging the precision of iTRAQ-MS quantification for individual proteins.

Insights into Heat-induced SUMOylation Provided by Quantitative Proteomics—Whereas our prior, non-quantitative MS study provided a glimpse into the dynamics of SUMOylation during heat stress in *Arabidopsis* (41), this iTRAQ-MS study provided a much richer appreciation of the process. As previously observed, the 172 substrates identified here are involved in diverse biological processes often associated with the nucleus (Table I). Notably, we could generate quantitative data for the entire collection of targets at all time points, strongly suggesting that they were all SUMOylated both before and after heat stress. Although we sometimes failed to detect an iTRAQ reporter peak above our cutoff value for specific peptides at one or more time points during individual MS/MS experiments, these rare absences only modestly affected the combined data from all peptides from a protein assessed in all replicates (supplemental Dataset S2). As an example, the quantification of the SUMO target IDN2 involved a combination of 78 peptide identifications; 71 had a measureable iTRAQ reporter peak at all four time points, 6 had no iTRAQ reporter peaks that met the cutoff threshold, and a single peptide had significant 114, 115, and 116 peaks but was missing the 117 peak. Another possible reason for widespread detection was precursor interference from impurities that could artifactually add values to individual reporter peaks

TABLE I
Effect of heat stress on representative SUMOylation targets[a]

	Name	Locus	Seq Cov %	# PSMs	Fold Increase 0.5	1.5	4	Description
Top 20 Increased	RPS35	At4g25500	21.7	41	16.9	17.6	2.6	RNA-splicing factor
	MORC	At5g50780	3.7	11	17.1	7.9	1.4	HsMORC4 homolog
	none	At1g54440	23.0	67	15.9	6.7	1.4	RNA helicase/exonuclease
	U2AF65A[b]	At4g36690	7.3	15	13.5	13.6	2.2	RNA-splicing factor
	PRH75	At5g62190	10.2	25	11.7	12.2	2.1	DEAD-Box RNA helicase 75
	IDN2	At3g48670	35.4	158	13.1	10.1	1.8	RNA-direct DNA methylation
	PUB49	At5g67530	10.8	36	12.1	7.2	1.4	Plant U-Box 49
	NRP1	At1g74560	15.8	15	9.9	11.6	2.6	Histone-binding protein
	none	At3g48060	10.1	95	10.8	8.7	1.5	Bromo-adjacent homology
	POLD3	At1g78650	7.2	32	10.0	10.7	2.3	DNA-direct DNA polymerase
	EML3	At5g13020	20.2	51	10.6	7.7	1.5	ENT/plant Tudor-like
	HSFA2	At2g26150	7.5	17	4.3	9.9	3.3	HS transcription factor
	CCR2	At2g21660	23.5	17	8.4	9.6	2.3	RNA-binding protein
	EFE	At1g05010	7.7	17	9.1	5.4	0.8	Ethylene-forming enzyme
	LA1	At4g32720	31.8	85	6.0	9.0	2.9	RNA-binding protein
	RSP41	At5g52040	19.4	43	7.0	8.7	1.6	RNA-splicing factor
	none[b]	At3g26560	1.8	9	8.2	8.7	1.9	pre-mRNA splicing factor
	STA1	At4g03430	28.7	139	8.3	7.9	1.6	RNA-splicing factor
	NUC-L1	At1g48920	13.0	40	6.2	8.3	1.8	rRNA-processsing factor
	none	At5g38840	7.4	14	5.8	8.0	1.9	SMAD+FHA domain
Other Notable Increased	SDN3[b]	At5g67240	9.0	25	7.8	7.5	2.1	Small RNA nuclease 3
	IMPA-6	At1g02690	22.4	43	7.0	4.8	1.6	Importin-alpha
	TFIIB	At2g41630	15.7	12	7.7	7.5	1.5	Transcription initiation factor
	BET9	At5g14270	8.5	41	7.9	6.4	1.7	Bromodomain-containing
	SIZ1	At5g60410	32.6	180	7.3	3.6	1.1	SUMO E3 enzyme
	PHR1	At4g28610	6.4	9	5.5	7.3	1.6	PO4 response trans. factor
	ADA2A	At3g07740	3.7	7	6.1	4.8	0.9	Transcription reg. factor
	TFIIS	At2g38560	10.5	17	5.3	6.5	1.9	Transcription elong. factor
	PKL	At2g25170	14.9	65	5.7	5.3	1.5	Chromatin remodeling
	GTL1	At1g33240	11.1	56	4.7	6.4	1.3	Transcription factor
	Ubiquitin	At2g47110	50.6	155	5.3	6.5	1.6	Post-translational modifier
	GTE3	At1g73150	10.6	26	4.9	3.4	0.9	Transcription factor
	TOPLESS	At1g15750	17.8	109	4.9	3.4	1.0	Transcription co-repressor
	HSFA1E	At3g02990	4.3	7	4.2	3.8	1.1	HS transcription factor
	GCN5	At3g54610	21.9	49	4.2	4.3	1.2	Histone acetyltransferase
	KU80[b]	At1g48050	11.0	25	3.9	4.1	1.3	DNA repair/telomere-related
	SEU	At1g43850	12.4	45	3.9	3.9	1.3	AGAMOUS co-regulator
	HUA2	At5g23150	2.7	20	4.0	4.2	1.3	Enhancer fo AG4-2 trans fac.
	ADA2B	At4g16420	15.5	41	3.6	3.6	1.2	Transcription reg. subunit
Notable Static /Decreased	HSFB2B	At4g11660	11.9	28	1.5	2.3	1.4	HS transcription factor
	SUVR1	At1g04050	7.8	16	2.0	2.0	1.0	Chromatin-remodeling factor
	SAE2[c]	At2g21470	35.7	96	1.6	1.9	1.1	SUMO E1 enzyme
	SUVR2[c]	At5g43990	32.8	105	1.5	1.7	1.1	Chromatin-remodeling factor
	SCE1[c]	At3g57870	48.8	19	1.0	1.2	0.8	SUMO E2 enzyme
	histone H2B	At5g02570	23.5	42	0.5	0.6	0.7	Nucleosome assembly

>7 | 7-4 | <4-2 | <2->0.5 | ≤0.5 Fold Increase

[a] Unless marked otherwise, normalized fold changes at $t = 0.5$ and 1.5 h are significantly different from $t = 0$ h (p values < 0.05).

[b] p values > 0.05 and < 0.1 for $t = 0.5$ and/or 1.5 h as compared to $t = 0$ h.

[c] p values ≥ 0.1 for $t = 0.5$ and/or 1.5 h as compared to $t = 0$ h.

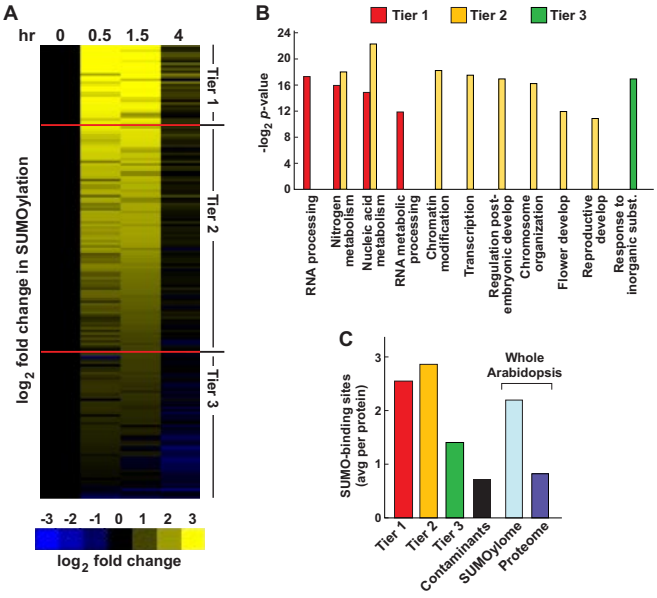

FIG. 4. **Dynamics and functional analysis of SUMO substrates during and after heat shock as quantified via iTRAQ MS.** *A*, relative changes in the SUMOylation status of 172 targets before and immediately after a 30-min heat shock at 37 °C followed by recovery at 24 °C. The values are illustrated by a heat map in which yellow denotes an increase in SUMOylation and blue denotes a decrease. The three tiers cluster proteins displaying a >7-fold increase (Tier 1), a 2- to 7-fold increase (Tier 2), or a <2-fold increase (Tier 3) in SUMOylation during the heat stress. *B*, GO functional enrichment for the targets clustered in each tier as a function of the $-\log_2(p \text{ value})$. *C*, the average number of high-probability ΨKxE SUMO-binding sites predicted per protein for each tier. The averages calculated for the collection of 59 contaminants isolated from wild-type plants, for the more complete *Arabidopsis* SUMOylome catalogue of 357 targets identified by Miller *et al.* (41), and for the entire *Arabidopsis* proteome were included for comparison.

(52, 54). However, our ability to detect with high accuracy both 6His-SUMO2 and a large collection of *Arabidopsis* proteins present in predefined amounts suggests that this interference is not prevalent for most proteins in our dataset (Fig. 2). Support for the idea that the quantitative data likely represent changes in SUMOylation occurring *in planta* was also provided by analysis of the set of 46 contaminants. Whereas the levels of SUMO conjugates often changed significantly during the heat-stress time course, levels of the contaminants remained relatively static (Fig. 3*E* and supplemental Fig. S3*A*). For example, 95% of the contaminant population was unaffected by the heat stress and displayed fold changes only between 0.44- and 1.537-fold after 30 min of the stress (supplemental Fig. S3*A*).

Consistent with the global increase in SUMOylated proteins during heat stress (~6-fold (Fig. 1*B*)), the SUMOylation state of most targets increased; 113 proteins experienced a ≥2-fold increase in SUMOylation after either 0.5 or 1.5 h, 32 of which increased by >7-fold to as much as 17-fold (Fig. 4*A*). Although cluster analysis based on kinetics failed to bin the SUMOylated collection into coherent groups, we noticed in repeated trials that the SUMOylation of some targets rose and fell sharply after heat shock, whereas others retained their SUMO tags longer upon return to the non-stress temperature (see Fig. 5 and Table I for examples).

Strikingly, the list of SUMOylated targets most strongly up-regulated by heat shock (>7-fold) were significantly enriched in proteins either known or predicted by GO annotations to participate in processes related to RNA, including RNA splicing, transport, and turnover and RNA-dependent DNA modification (Tier 1: Figs. 4*A* and 4*B*, Table I). Notable examples were the RNA splicing/degrading/helicase proteins RSP35, RSP41, PRH75, U2AF65A, SDN3, STA1, and NUCL1; the RNA binding proteins LA1 and CCR2; and the RNA-dependent DNA methylation-related protein IDN2. Non-RNA-related factors experiencing strong increases in SUMOylation state (>7-fold) after heat stress included the heat shock transcription factor HSF2A, a previously identified SUMO target known to be important for establishing long-term acquired thermotolerance (27, 41, 55). Also among the Tier 1 targets was an *Arabidopsis* ortholog of the mammalian SIM-containing DNA gyrase MORC involved in heterochromatin condensation and transcriptional repression (56, 57), the POLD3 DNA polymerase core subunit, and the histone-binding protein NRP1.

The collection of moderately up-regulated targets (7- to ≥2-fold) were enriched for a more diverse range of functions primarily associated with the nucleus (Tier 2: Figs. 4*A* and 4*B*, Table I). Included were factors involved in chromatin maintenance (*e.g.* PKL, ADA2A, GCN5, and KU80), as well as several DNA polymerase subunits (TFIIB and TFIIS) and a host of transcription factors and co-regulators (*e.g.* HSFA1E, PHR1, SEU, BET9, GTE3, and TOPLESS). In addition to the strongly affected targets, we identified a suite of proteins whose SUMOylation status was unaltered by heat shock (Tier 3: Fig. 4*A*). Although it is possible that some in the Tier 3 collection are contaminants, the facts they were often detected by high PSM counts, they were enriched for the ΨKxE SUMO-binding motif (1.37 motifs per protein, compared with 0.75 for contaminants (Fig. 4*C*)), and/or they or their likely orthologs were identified previously as SUMO targets in *Arabidopsis* and other organisms (*e.g.* SUVR1, SUVR2, SAE2, and SCE1 (20, 41)) argue that they are real SUMO substrates. The robust constitutive SUMOylation of some targets suggests that their modification is regulated by a SUMO E3 and/or deSUMOylating protease not shared with the heat-stress-regulated targets.

In contrast to the above examples, we discovered three *Arabidopsis* proteins whose SUMOylation status dropped significantly during heat stress (>2-fold). Of most interest was the histone H2B protein encoded by the At4g16420 loci, which experienced a ~2-fold drop in SUMOylation state soon after heat stress (0.5 h) but rebounded after a 3.5-h recovery (Table I). In agreement, mammalian histone H2B was recently reported to be similarly deSUMOylated after heat stress (20)

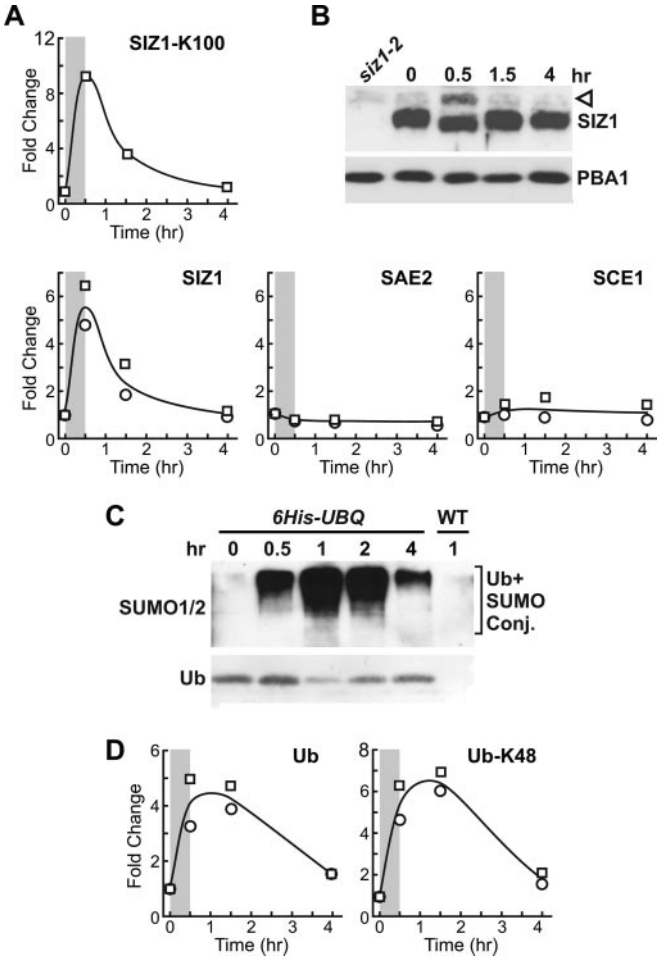

FIG. 5. **SUMOylation of SIZ1 and the ubiquitylation of SUMO1/2 targets increase dramatically and reversibly during heat shock.** Seedlings were collected before and immediately after a 30-min heat shock at 37 °C (shaded areas) followed by recovery at 24 °C. *A*, relative changes in the SUMOylation status for SIZ1, SAE2, and SCE1 as quantified via iTRAQ MS. SIZ1-K100 represents SIZ1 peptides bearing a SUMO footprint at K100. *B*, change in the SUMOylation status of SIZ1 as determined via immunoblot analysis of total protein extracts with anti-SIZ1 antibodies. The arrowhead identifies the SUMO-SIZ1 conjugate. Immunoblot analysis with anti-PBA1 antibodies was used to confirm equal protein loading. Sample from a non-stressed *siz1–2* seedling was included to identify SIZ1. *C*, increases in the abundance of Ub+SUMO1/2 conjugates. Ub conjugates were purified from *6His-UBQ*-expressing plants by means of Ni-NTA chromatography and were subjected to immunoblot analysis with anti-SUMO1 antibodies. Protein extracts enriched via Ni-NTA chromatography from wild-type plants at $t = 1$ h were included as a control. The region of the gel containing free 6His-Ub is also shown. *D*, relative changes in the abundance of Ub+SUMO1 conjugates in *6His-SUMO1-H89R sumo1–1 sumo2–1* plants first enriched for SUMO1 and then quantified via iTRAQ MS. iTRAQ values for all Ub peptides and the Ub peptide bearing a Ub footprint at K48 are shown (Ub-K48). When possible, the average fold change values for two independent biological replicates were included.

Identification of SUMO1 Binding Sites—The H89R substitution engineered into the 6His-SUMO1-H89R variant was designed to simplify MS identification of SUMO1/2 binding sites by reducing the length of the SUMO footprint generated after trypsinization from 25 residues to just the short QTGG sequence isopeptide linked to a non-cleaved lysine (41). Whereas standard MS/MS analyses previously detected a number of footprints with the signature K^+343 or K^+326 *m/z* fragmentations (QTGG, in which Q was unmodified or cyclized, respectively (41)), SEQUEST searches of the iTRAQ-MS spectra were much less successful. One complication we found is that the N-terminus of the SUMO1-H89R footprint also reacts with the isobaric tag in addition to the N-terminus of the target peptide. Unfortunately, searches for such dual iTRAQ-modified peptides yielded little improvement, suggesting that the isobaric tags sufficiently complicate database searches, possibly by adding new fragmentation patterns that cannot be interpreted by standard MS analysis software. Despite these problems, we successfully quantified the abundance of a few SUMO1 linkages during heat stress, the most notable of which was SUMO1 linked to K100 of SIZ1 detected previously (41) (supplemental Fig. S5*A*). We also quantified a Ub footprint (K^+GG, 114 *m/z*) peptide involving the modification of Ub itself at K48 as a signature for the presence of K48-linked poly-Ub chains in our SUMO conjugate preparations (supplemental Fig. S5*B*). The presence of these Ub chains could reflect SUMO targets in which lysines other than those directly SUMOylated became poly-ubiquitylated, or targets in which the bound SUMO moieties themselves provided the initiation sites for assembling poly-Ub chains.

Confirmation of SUMOylation Targets—Components of the SUMO system itself are commonly found in the proteomic catalogs of SUMOylated proteins (20, 58, 59), which for *Arabidopsis* currently include the E1 subunit SAE2, the SCE1 E2, the SIZ1 E3, and the ESD4 SUMO protease (41). Our quantitative dataset revealed that the SUMOylation state of SIZ1, but not SAE2 and SCE1, within the conjugation pathway strongly increases after heat stress (~7-fold up), and this was supported by the iTRAQ-MS analysis of the tryptic peptide containing the SUMO1-H89R footprint (QTGG) at K100, as well as several other non-modified SIZ1 peptides (Fig. 5*A*). To help confirm this result, we generated antibodies against SIZ1 and used them to probe crude extracts obtained from wild-type seedlings exposed to the heat-stress time course. As shown in Fig. 5*B*, a new species recognized by anti-SIZ1 antibodies at the appropriate mass for a SUMO1/2-SIZ1 conjugate was detected 30 min after the start of the heat-stress time course but was absent before or after, in line with the sharp rise and fall determined by iTRAQ MS.

Quantitative iTRAQ-MS analysis of a tryptic peptide containing the Ub footprint (GG) at K48, as well as other Ub peptides, supported previous MS studies showing that a subset of SUMOylated proteins also become robustly ubiquitylated during heat stress (20, 41, 42). Levels of these Ub peptides in *Arabidopsis* rapidly increased ~5- to 6-fold after a 30-min treatment at 37 °C and then slowly declined upon return to 24 °C (Fig. 5*D*). To confirm this response, we ex-

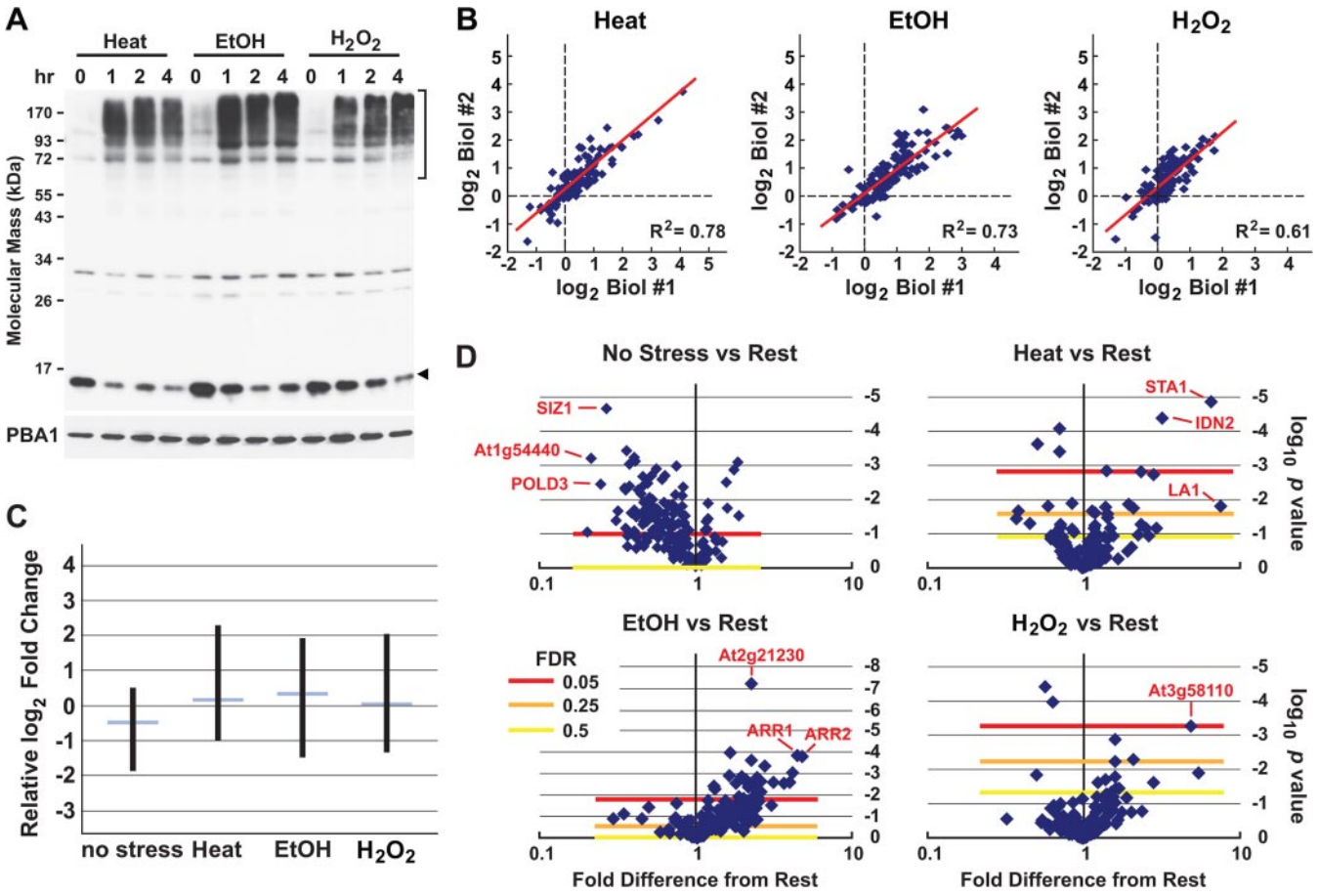

FIG. 6. **Comparison of the SUMOylation status of *Arabidopsis* targets affected by heat, ethanol, or oxidative (H_2O_2) stress using iTRAQ MS.** *A*, immunoblot analysis showing the rise in SUMO1/2 conjugates in seedlings exposed continuously to 37 °C, 10% ethanol, or 50 mM H_2O_2. Crude extracts subjected to SDS-PAGE were probed with anti-SUMO1 or anti-PBA1 (loading control) antibodies. *B*, reproducibility of the fold increase for the collection of 174 SUMOylated proteins between two biological replicates subjected continuously to 2 h of each stress. The $\log_2$ fold change represents the relative value at the end of the stress as compared with that at $t = 0$. The line of best fit linear regression (red), along with the corresponding R^2 value, is included in each panel. *C*, Whisker plots show the range of fold change values detected for each condition. Blue boxes indicate 95% confidence intervals of the means, whereas lines show the range between maximum and minimum fold change values. *D*, Volcano plots comparing the stress-specific fold change values for heat, ethanol, and H_2O_2 to all other values (both stressed and non-stressed) relative to the levels of FDR confidence in quantification value. Several proteins displaying significant stress-specific changes are indicated. Data and statistical analysis for all targets can be found in supplemental Dataset S3.

ploited a transgenic *Arabidopsis* line expressing 6His-Ub (50) to enrich by Ni-NTA chromatography for Ub conjugates during the heat shock time course and then assayed for the abundance of Ub+SUMO conjugates in these preparations by means of immunoblot analysis with anti-SUMO1 antibodies. In agreement with prior studies (41, 60), the total Ub conjugate pool rose only modestly upon heat stress, in contrast to the strong increase in SUMO1/2 conjugates (supplemental Fig. S6). Ub+SUMO conjugate levels observed immunologically after purification also rose substantially after heat stress with the overall kinetics congruent with the iTRAQ-MS values for the Ub-K48 footprint and other Ub peptides (Fig. 5*C*).

SUMOylation Response to Ethanol and Oxidative Stress—A number of other stressful conditions are known to induce the accumulation of SUMO conjugates in *Arabidopsis* and other eukaryotes, including high concentrations of ethanol and H_2O_2 (7, 41, 44, 61, 62). To examine whether a similar collection of targets also becomes strongly SUMOylated under these stresses, we directly compared, by means of iTRAQ MS, the profile of conjugates that accumulated after a continuous 2-h exposure to 37 °C, 10% ethanol, or 50 mM H_2O_2. Preliminary studies revealed that these conditions are not lethal to liquid-grown *Arabidopsis* seedlings based on their ability to remain viable and resume growth after a return to 24 °C, or after the medium is exchanged for one missing the chemical. As was seen with heat treatments, 7-day-old *6His-SUMO1-H89R sumo1–1 sumo2–1* seedlings treated with either chemical strongly increased their levels of SUMO1 conjugates as determined via immunoblot analysis, with their overall profiles of conjugates indistinguishable from those seen after heat treatment (Fig. 6*A*). Following affinity purifica-

tion and iTRAQ labeling in the presence of the 6His-SUMO2 standard (Fig. 1*D* and supplemental Fig. S1*B*), the relative abundance of individual SUMO1 conjugates was directly compared with their abundance in control seedlings. Only those targets identified by two or more peptides in each biological replicate were included in the subsequent analysis.

Using the criteria established above, we successfully compared the levels of 174 SUMO substrates before and after the three treatments. Supporting experimental reproducibility, quantification values were positively correlated between biological repeats of the same stress conditions ($R^2 = 0.78$, 0.73, and 0.61 for heat *versus* heat, EtOH *versus* EtOH, and H_2O_2 *versus* H_2O_2, respectively) (Fig. 6*B*). In general, heat, ethanol, and H_2O_2 induced an overall increase in SUMOylation; the mean fold change of each stress condition was significantly elevated relative to the non-stress condition and to the fold change values of contaminants (Fig. 6*C* and supplemental Fig. S3*B*). Collectively, the SUMOylation status of 77% of the identified targets (134 total) was statistically affected by one or more stresses relative to the non-stressed condition (FDR < 0.05), with most strongly up-regulated. As shown by the heat maps and cross comparisons in Fig. 6*D* and supplemental Figs. S7*A* and S7*B*, a core group of SUMO targets was similarly affected by all stress treatments, and a smaller subset of targets showed stress-specific regulation. In fact, the linear regression R^2 values revealed that for the core group comprising 86% of targets, correlations existed between the heat and ethanol, heat and H_2O_2, and ethanol and H_2O_2 datasets ($R^2 = 0.65$, 0.53, and 0.53, respectively (supplemental Fig. S7*A*)). As with heat stress, there was an enrichment for proteins known or predicted to be involved in RNA biology (supplemental Dataset S3). Individual examples of proteins strongly SUMOylated by all three stresses include transcription factors (*e.g.* HUA2, SEU, and HAG1), the POLD3 DNA polymerase core subunit, the PRH75 RNA helicase, and the SUMO E3 SIZ1.

We also found a subset of SUMO targets that appeared to be differentially regulated by the three stresses, with a number showing statistically significant up-regulation relative to all other conditions (Fig. 6*D*). Chief among these targets were IDN2, LA1, and STA1, which were more affected by heat stress; the PHR1, BLH7, and UNE1 transcription factors and the *Arabidopsis* response regulators ARR1 and ARR2, which were more affected by ethanol; and ascorbate peroxidase, which was selectively SUMOylated upon H_2O_2 treatment (Fig. 6*D* and supplemental Fig. S7*B*). The effect on ascorbate peroxidase is particularly noteworthy given its role in oxidative stress protection, which involves catalyzing the cytosolic breakdown of H_2O_2 (63). An additional analysis directly comparing treatments in pairs found 23 proteins that were more than 2 S.D.s from the mean fold change ratio (supplemental Fig. S7*B*). These outliers overlapped with the targets identified in the volcano plot analysis and were significantly enriched for the consensus ΨKxE SUMO-binding site (2.7 *versus* 2.5 sites per protein for the full list of 174 targets), suggesting that these proteins are in fact SUMO substrates and not stress-specific contaminants (supplemental Figs. S7*A*, S7*C*, and S7*D*).

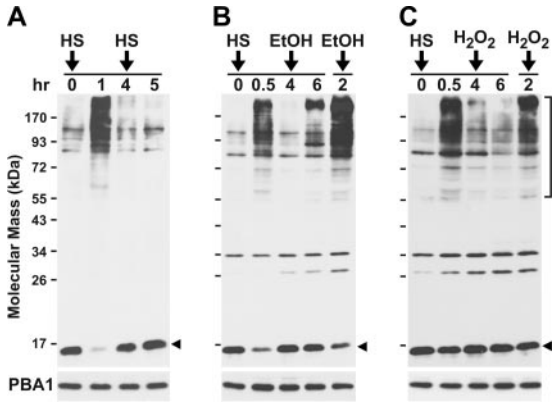

FIG. 7. **An initial heat shock dampens the rise in SUMOylation following subsequent exposure to heat, ethanol, or H_2O_2 stress.** Seedlings were exposed to an initial heat shock for 30 min at 37 °C and allowed to recover at 24 °C for 3.5 h before the second stress. Total protein extracts were subjected to immunoblot analysis with anti-SUMO1 antibodies and anti-PBA1 antibodies (loading control). *A*, seedling exposed to a second heat shock at 37 °C. *B*, *C*, seedlings exposed to a second stress of 10% ethanol (*B*) or 50 mM H_2O_2 (*C*) for 2 h. For comparison, samples from seedlings exposed to ethanol or H_2O_2 for 2 h without a prior heat shock were included on the right lanes of each gel. Arrowheads and bracket locate free and conjugated SUMO1/2, respectively.

A prominent feature of heat-stress-induced SUMOylation in *Arabidopsis* is its striking memory, whereby seedlings exposed to a second heat stress soon after the first will not up-regulate SUMOylation, although they will do so after many hours of recovery (7) (Fig. 7*A*). To further explore whether SUMOylation induced by ethanol or H_2O_2 stress is controlled by the same signaling system, we tested whether the refractory period induced by heat also impacted plants when applied as a second stress. Indeed, when wild-type plants were subjected to a 30-min 37 °C heat shock followed by a 3.5-h recovery period and then subsequently exposed for 2 h to ethanol or H_2O_2, the second response was substantially attenuated relative to that for naïve seedlings exposed for 2 h to ethanol or H_2O_2 alone (Figs. 7*B*, 7*C*). Therefore, although subtle differences in the SUMOylation response after heat, ethanol, and H_2O_2 are evident, the overall list of affected targets and at least some aspects of the signaling system underpinning these modifications are shared.

DISCUSSION

Mounting evidence indicates that SUMO is a crucial post-translational modifier that is essential for eukaryotes and key to their survival during stress. Using advanced proteomics combined with the iTRAQ method for quantification, we described kinetically how the SUMOylation state of an extensive list of *Arabidopsis* proteins is affected by heat, ethanol, and

H_2O_2 stress. The advantages of using iTRAQ over other MS quantification methods such as SILAC were our ability to analyze an intact organism without the complications of metabolic labeling (which is especially problematic for plants) and the ability to measure multiple time points/samples simultaneously. High accuracy was achieved with the use of spiked 6His-SUMO2 to adjust for sample-to-sample variations during purification and iTRAQ labeling, and by focusing on targets with two or more PSMs from which to extract quantitative data. Based on the MS analysis of a dilution series of SUMO1 conjugates spiked with 6His-SUMO2, our iTRAQ methodology provided reasonably accurate quantification from 2- to at least 16-fold changes for the heterogeneous mix of SUMO targets analyzed here without substantial precursor ion interference from contaminants (Fig. 2). One surprising finding from this study was that all 172 proteins in our final dataset for heat stress appeared to be SUMOylated at all times. Thus, stress appears to enhance the SUMOylation status for many targets that are modified before the stress, as opposed to directing the modification of a new set of targets. However, given that that catalogue of 172 targets likely includes the most robustly SUMOylated targets (Fig. 3*G*), we cannot rule out the possibility that other targets at lower abundance show strong stress specificity.

Consistent with our previous proteomic analysis of *Arabidopsis* (41) and with analyses by others using yeast and mammalian cell cultures (14, 15, 20, 42, 64), we found that stress increases the SUMOylation state of a number of predominantly nuclear substrates that affect a wide range of nuclear events. Processes highlighted by our study as being heavily influenced by stress-induced SUMOylation center on RNA homeostasis, with some of the most dynamically up-regulated targets (13 of 34 targets increased by >7-fold, Tier 1) known or predicted to be involved in RNA binding, splicing, end processing and polyadenylation, and/or turnover (65). Taken together, our data strongly suggest that SUMOylation globally impacts post-transcriptionally important features of the transcriptome. As such, SUMOylation could play a crucial role in modifying the mRNA profile during stress to encourage the accumulation of stress-related transcripts, or to discourage the accumulation of transcripts more important under normal growth conditions (*e.g.* rRNAs) or transcripts derived from transposons that might become active during stress (36, 66, 67).

One of the more dynamic targets in our *Arabidopsis* dataset is IDN2, a double-stranded RNA-binding protein that controls both *de novo* methylation and small-interfering RNA-mediated maintenance methylation (68). Its robust SUMOylation during heat stress (~13-fold up) might reflect SUMO-mediated control of DNA methylation patterns, which, together with the stress-up-regulated SUMOylation of *Arabidopsis* versions of MORC (~17-fold up) and histone acetylases/deacetylases such as GCN5/ADA2B (6-fold/4-fold up) and HDA19 (41; this report), might then help convert euchromatic regions into heterochromatic regions during stress (57). Previous studies have connected SUMOylation to mRNA export, including the findings that the major plant SUMO protease ESD4 is localized to the *Arabidopsis* nuclear pore and that the *esd4-1* null mutant displays increased nuclear RNA retention (16, 69, 70). Our proteomics datasets offer a collection of dynamically affected RNA-binding SUMO substrates that might be responsible for this retention.

Another potentially important mechanism by which SUMOylation could affect stress tolerance is the activation of heat shock transcription factors (HSFs) and other transcriptional regulators/co-regulators. We identified three HSFs as being SUMO targets (41; this report); principal among these is HSFA2, whose SUMOylation state rapidly increased ~10-fold following heat stress. Prior studies with related HSFs in mammalian cells showed that their heat-shock-stimulated SUMOylation affects binding to their cognate promoter elements, although the direction of the response remains in question (71–73). Given the role of HSFA2 in the establishment of acquired thermotolerance, it is tempting to speculate that its SUMOylation not only is involved in basal stress tolerance (7, 28), but also serves as a guard against future insults (27).

It is interesting to note that stress also induces the ubiquitylation of a subset of *Arabidopsis* SUMO targets. Prior MS analyses revealed that SUMO1 itself is a substrate and that K48-poly-Ub chains become prevalent in the SUMO1/2 conjugate pool, indicating that at least some Ubs are attached as poly-Ub chains, with the added possibility that these chains are directly linked to previously bound SUMO1/2 moieties (41). The transient accumulation of Ub+SUMO1/2 conjugates during heat stress and the likely presence of poly-Ub chains linked internally via K48 might reflect the action of the SUMO1/2 moieties as secondary degrons in stimulating the Ub/26S proteasome-mediated turnover of proteins following stress. The increase in ubiquitylated SUMO conjugates seen after treating mammalian cells with the proteasome inhibitor MG132 is consistent with this proteolytic role (42). Several SUMO-dependent Ub E3s that drive this dual modification have been described in yeast and mammals (74, 75), likely orthologs of which are encoded within the *Arabidopsis* genome.

Of particular importance to understanding the functions of SUMO is an appreciation of the mechanism(s) underlying its stress-induced up-regulation. Toward this end, our data provide several new insights. First, based on the highly overlapping sets of targets robustly SUMOylated upon heat, ethanol, and H_2O_2 exposure, it appears that a common signal transduction pathway is used to activate SUMOylation in response to these stresses. Given such, the affected targets might represent important players in general stress protection in plants and possibly other eukaryotes. This notion of a common pathway is further supported by an apparent shared memory that generates a general refractory period blocking

subsequent stress-induced SUMOylation for an extended time period after the initial challenge.

Second, our kinetic analyses imply that stress mostly increases the abundance of existing conjugates, as opposed to modifying new targets. As a consequence, it is tempting to speculate that stress-induced SUMOylation is underpinned by a relatively simple process that activates/inactivates the same conjugation/deconjugation machinery in operation before stress. Regulatory points proposed in metazoans include the ethanol-induced sequestration of the nuclear pore-associated SUMO protease ULP1 (62) and inactivation of mammalian SUMO proteases by high levels of oxidants (61). Here, we found that in plants exposed to stressful concentrations of ethanol or H_2O_2, the SUMOylation status of a set of proteins increased in a manner mostly similar to that elicited by heat. It is thus possible that plants employ a common SUMO protease inhibitory mechanism to increase SUMO1/2 conjugates globally when subjected to a range of stresses, and that this mechanism is overlaid by selective effects on one or more SUMO proteases to generate the variations in SUMOylation among the small subset of stress-specific targets.

Another regulatory hub in plants under stress might involve the SIZ1 E3, based on its central role in driving stress-induced SUMOylation and its importance to stress protection (6, 8, 25). Considering its consistent detection in SUMO conjugate preparations via MS and its routinely high PSM counts, SIZ1 appears to be one of the more abundant SUMOylated proteins in *Arabidopsis* (41), and unlike other components of the SUMOylation system examined, the SUMOylation state of SIZ1 rises substantially during heat stress (7-fold up soon after heat shock). The rise is remarkably transient, with the levels of SUMO1/2-SIZ1 conjugates dropping rapidly to basal levels after the seedlings have returned to a non-stress temperature, indicating that the bound SUMO moiety itself is not a long-lived signal. Two recent proteomic studies describing stress-induced SUMOylation in mammalian cells also identified a SIZ1-type SUMO E3 (PIAS) as strongly SUMOylated during stress, implying that this modification is conserved among eukaryotes and thus is of potential regulatory consequence (20, 59). One intriguing idea is that the stress-induced SUMOylation of SIZ1-type E3s helps dampen up-regulated SUMOylation during stress by the bound SUMO moiety or moieties either directly repressing the activity of the ligase or committing SUMOylated SIZ1 to ubiquitylation and subsequent turnover by the 26S proteasome. A more mundane alternative is that SIZ1 SUMOylation represents inadvertent transfer of the activated SUMO from the high energy SUMO-E2 intermediate to SIZ1 instead of to the target. This "collateral damage" would likely become more frequent as SIZ1 becomes more active during stress. In support, the E3s that direct Ub transfer are often targets of autoubiquitylation in the absence of substrates (76). Clearly, determining the effects of SUMOylation on the functions of individual targets like SIZ1 should help reveal how SUMO addition is induced by stress and confers protection in plants and other eukaryotes.

Acknowledgments—We thank Drs. Josh Coon, Justin Brumbaugh, and Michael Shortreed for helpful advice.

* This work was supported by NSF *Arabidopsis* 2010 (MCB-0929100) and Plant Genome EAGER Program (IOS-1232752) grants to R.D.V., an NIH-sponsored predoctoral training fellowship to the UW Genetics Training Program (to M.J.M.), and grants from NIH/NHGRI (1P50HG004952) and NIH-NIGMS (P01GM081629) to M.S. and L.M.S.

S This article contains supplemental material.

¶ To whom correspondence should be addressed: Dr. Richard D. Vierstra, Department of Genetics, 425-G Henry Mall, University of Wisconsin, Madison, WI 53706, Tel.: 608–262-8215, Fax: 608–262-2976, E-mail: vierstra@wisc.edu.

REFERENCES

1. Yamaguchi-Shinozaki, K., and Shinozaki, K. (2006) Transcriptional regulatory networks in cellular responses and tolerance to dehydration and cold stresses. *Ann. Rev. Plant Biol.* **57,** 781–803
2. Jones, J. D. G., and Dangl, J. L. (2006) The plant immune system. *Nature* **444,** 323–329
3. Richter, K., Haslbeck, M., and Buchner, J. (2010) The heat shock response: life on the verge of death. *Mol. Cell* **40,** 253–266
4. Wilkinson, K. A., and Henley, J. M. (2010) Mechanisms, regulation and consequences of protein SUMOylation. *Biochem. J.* **428,** 133–145
5. Geiss-Friedlander, R., and Melchior, F. (2007) Concepts in SUMOylation: a decade on. *Nat. Rev. Mol. Cell Biol.* **8,** 947–956
6. Miura, K., Jin, J. B., and Hasegawa, P. M. (2007) SUMOylation, a post-translational regulatory process in plants. *Curr. Opin. Plant Biol.* **10,** 495–502
7. Kurepa, J., Walker, J. M., Smalle, J., Gosink, M. M., Davis, S. J., Durham, T. L., Sung, D. Y., and Vierstra, R. D. (2003) The small ubiquitin-like modifier (SUMO) protein modification system in *Arabidopsis*. Accumulation of SUMO1 and -2 conjugates is increased by stress. *J. Biol. Chem.* **278,** 6862–6872
8. Saracco, S. A., Miller, M. J., Kurepa, J., and Vierstra, R. D. (2007) Genetic analysis of SUMOylation in *Arabidopsis*: conjugation of SUMO1 and SUMO2 to nuclear proteins is essential. *Plant Physiol.* **145,** 119–134
9. Miura, K., Rus, A., Sharkhuu, A., Yokoi, S., Karthikeyan, A. S., Raghothama, K. G., Baek, D., Koo, Y. D., Jin, J. B., Bressan, R. A., Yun, D. J., and Hasegawa, P. M. (2005) The *Arabidopsis* SUMO E3 ligase SIZ1 controls phosphate deficiency responses. *Proc. Natl. Acad. Sci. U.S.A.* **102,** 7760–7765
10. Ishida, T., Fujiwara, S., Miura, K., Stacey, N., Yoshimura, M., Schneider, K., Adachi, S., Minamisawa, K., Umeda, M., and Sugimoto, K. (2009) SUMO E3 ligase HIGH PLOIDY2 regulates endocycle onset and meristem maintenance in *Arabidopsis*. *Plant Cell* **21,** 2284–2297
11. Huang, L., Yang, S., Zhang, S., Liu, M., Lai, J., Qi, Y., Shi, S., Wang, J., Wang, Y., Xie, Q., and Yang, C. (2009) The *Arabidopsis* SUMO E3 ligase AtMMS21, a homologue of NSE2/MMS21, regulates cell proliferation in the root. *Plant J.* **60,** 666–678
12. Rodriguez, M. S., Dargemont, C., and Hay, R. T. (2001) SUMO-1 conjugation *in vivo* requires both a consensus modification motif and nuclear targeting. *J. Biol. Chem.* **276,** 12654–12659
13. Matic, I., Schimmel, J., Hendriks, I. A., van Santen, M. A., van de Rijke, F., van Dam, H., Gnad, F., Mann, M., and Vertegaal, A. C. O. (2010) Site-specific identification of SUMO-2 targets in cells reveals an inverted SUMOylation motif and a hydrophobic cluster SUMOylation motif. *Mol. Cell* **39,** 641–652
14. Bruderer, R., Tatham, M. H., Plechanovova, A., Matic, I., Garg, A. K., and Hay, R. T. (2011) Purification and identification of endogenous poly-SUMO conjugates. *EMBO Rep.* **12,** 142–148
15. Matic, I., van Hagen, M., Schimmel, J., Macek, B., Ogg, S. C., Tatham, M. H., Hay, R. T., Lamond, A. I., Mann, M., and Vertegaal, A. C. (2008) In vivo identification of human small ubiquitin-like modifier polymerization sites by high accuracy mass spectrometry and an *in vitro* to *in vivo*

strategy. *Mol. Cell. Proteomics* **7,** 132–144
16. Murtas, G., Reeves, P. H., Fu, Y. F., Bancroft, I., Dean, C., and Coupland, G. (2003) A nuclear protease required for flowering-time regulation in *Arabidopsis* reduces the abundance of small ubiquitin-related modifier conjugates. *Plant Cell* **15,** 2308–2319
17. Conti, L., Price, G., O'Donnell, E., Schwessinger, B., Dominy, P., and Sadanandom, A. (2008) Small ubiquitin-like modifier proteases OVERLY TOLERANT TO SALT1 and -2 regulate salt stress responses in *Arabidopsis. Plant Cell* **20,** 2894–2908
18. Hermkes, R., Fu, Y. F., Nurrenberg, K., Budhiraja, R., Schmelzer, E., Elrouby, N., Dohmen, R. J., Bachmair, A., and Coupland, G. (2011) Distinct roles for *Arabidopsis* SUMO protease ESD4 and its closest homolog ELS1. *Planta* **233,** 63–73
19. Saitoh, H., and Hinchey, J. (2000) Functional heterogeneity of small ubiquitin-related protein modifiers SUMO-1 versus SUMO-2/3. *J. Biol. Chem.* **275,** 6252–6258
20. Golebiowski, F., Matic, I., Tatham, M. H., Cole, C., Yin, Y., Nakamura, A., Cox, J., Barton, G. J., Mann, M., and Hay, R. T. (2009) System-wide changes to SUMO modifications in response to heat shock. *Sci. Signal.* **2,** ra24
21. Tanaka, K., Nishide, J., Okazaki, K., Kato, H., Niwa, O., Nakagawa, T., Matsuda, H., Kawamukai, M., and Murakami, Y. (1999) Characterization of a fission yeast SUMO-1 homologue, Pmt3p, required for multiple nuclear events, including the control of telomere length and chromosome segregation. *Mol. Cell. Biol.* **19,** 8660–8672
22. Johnson, E. S., Schwienhorst, I., Dohmen, R. J., and Blobel, G. (1997) The ubiquitin-like protein Smt3p is activated for conjugation to other proteins by an Aos1p/Uba2p heterodimer. *EMBO J.* **16,** 5509–5519
23. Seufert, W., Futcher, B., and Jentsch, S. (1995) Role of a ubiquitin-conjugating enzyme in degradation of S- and M-phase cyclins. *Nature* **373,** 78–81
24. Catala, R., Ouyang, J., Abreu, I. A., Hu, Y., Seo, H., Zhang, X., and Chua, N. H. (2007) The *Arabidopsis* E3 SUMO ligase SIZ1 regulates plant growth and drought responses. *Plant Cell* **19,** 2952–2966
25. Miura, K., Jin, J. B., Lee, J., Yoo, C. Y., Stirm, V., Miura, T., Ashworth, E. N., Bressan, R. A., Yun, D. J., and Hasegawa, P. M. (2007) SIZ1-mediated SUMOylation of ICE1 controls CBF3/DREB1A expression and freezing tolerance in *Arabidopsis. Plant Cell* **19,** 1403–1414
26. Park, B. S., Song, J. T., and Seo, H. S. (2011) *Arabidopsis* nitrate reductase activity is stimulated by the E3 SUMO ligase AtSIZ1. *Nat. Commun.* **2,** 400
27. Cohen-Peer, R., Schuster, S., Meiri, D., Breiman, A., and Avni, A. (2010) SUMOylation of *Arabidopsis* heat shock factor A2 (HsfA2) modifies its activity during acquired thermotholerance. *Plant Mol. Biol.* **74,** 33–45
28. Yoo, C. Y., Miura, K., Jin, J. B., Lee, J., Park, H. C., Salt, D. E., Yun, D. J., Bressan, R. A., and Hasegawa, P. M. (2006) SIZ1, small ubiquitin-like modifier E3 ligase facilitates basal thermotolerance in *Arabidopsis* independent of salicylic acid. *Plant Physiol.* **142,** 1548–1558
29. van den Burg, H. A., Kini, R. K., Schuurink, R. C., and Takken, F. L. W. (2010) *Arabidopsis* small ubiquitin-like modifier paralogs have distinct functions in development and defense. *Plant Cell* **22,** 1998–2016
30. Lee, J., Nam, J., Park, H. C., Na, G., Miura, K., Jin, J. B., Yoo, C. Y., Baek, D., Kim, D. H., Jeong, J. C., Kim, D., Lee, S. Y., Salt, D. E., Mengiste, T., Gong, Q., Ma, S., Bohnert, H. J., Kwak, S. S., Bressan, R. A., Hasegawa, P. M., and Yun, D. J. (2007) Salicylic acid-mediated innate immunity in *Arabidopsis* is regulated by SIZ1 SUMO E3 ligase. *Plant J.* **49,** 79–90
31. Miura, K., Lee, J., Jin, J. B., Yoo, C. Y., Miura, T., and Hasegawa, P. M. (2009) SUMOylation of ABI5 by the *Arabidopsis* SUMO E3 ligase SIZ1 negatively regulates abscisic acid signaling. *Proc. Natl. Acad. Sci. U.S.A.* **106,** 5418–5423
32. Miura, K., Lee, J., Miura, T., and Hasegawa, P. M. (2010) SIZ1 controls cell growth and plant development in *Arabidopsis* through salicylic acid. *Plant Cell Physiol.* **51,** 103–113
33. Lois, L. M., Lima, C. D., and Chua, N. H. (2003) Small ubiquitin-like modifier modulates abscisic acid signaling in *Arabidopsis. Plant Cell* **15,** 1347–1359
34. Ponder, E. L., Albrow, V. E., Leader, B. A., Bekes, M., Mikolajczyk, J., Fonovic, U. P., Shen, A., Drag, M., Xiao, J., Deu, E., Campbell, A. J., Powers, J. C., Salvesen, G. S., and Bogyo, M. (2011) Functional characterization of a SUMO deconjugating protease of *Plasmodium falciparum* using newly identified small molecule inhibitors. *Chem Biol.* **18,** 711–721
35. Lee, Y. J., Mou, Y., Maric, D., Klimanis, D., Auh, S., and Hallenbeck, J. M. (2011) Elevated global SUMOylation in Ubc9 transgenic mice protects their brains against focal cerebral ischemic damage. *PLoS One* **6,** e25852
36. Kessler, J. D., Kahle, K. T., Sin, T., Meerbrey, K. L., Schlabach, M. R., Schmitt, E. M., Skinner, S. O., Xu, Q., Li, M. Z., Hartman, Z. C., Rao, M., Yu, P., Dominquez-Vidana, R., Liang, A. C., Solimini, N. L., Bernardi, R. J., Yu, B., Hsu, T., Golding, I., Luo, J., Osborne, C. K., Creighton, C. J., Hilsenbeck, S. G., Schiff, R., Shaw, C. A., Elledge, S. J., and Westbrook, T. F. (2012) The SUMOylation-dependent transcriptional subprogram is required for Myc-driven tumorigenesis. *Science* **335,** 348–353
37. Wimmer, P., Schreiner, S., and Dobner, T. (2012) Human pathogens and the host cell SUMOylation system. *J. Virol.* **86,** 642–654
38. Sanchez-Duran, M. A., Dallas, M. B., Ascencio-Ibanez, J. T., Reyes, M. I., Arroyo-Mateos, M., Ruiz-Albert, J., Hanley-Bowdoin, L., and Bejarano, E. R. (2011) Interaction between geminivirus replication protein and the SUMO-conjugating enzyme is required for viral infection. *J. Virol.* **85,** 9789–9800
39. Hecker, C. M., Rabiller, M., Haglund, K., Bayer, P., and Dikic, I. (2006) Specification of SUMO1- and SUMO2-interacting motifs. *J. Biol. Chem.* **281,** 16117–16127
40. Song, J., Durrin, L. K., Wilkinson, T. A., Krontiris, T. G., and Chen, Y. (2004) Identification of a SUMO-binding motif that recognizes SUMO-modified proteins. *Proc. Natl. Acad. Sci. U.S.A.* **101,** 14373–14378
41. Miller, M. J., Barrett-Wilt, G. A., Hua, Z., and Vierstra, R. D. (2010) Proteomic analyses identify a diverse array of nuclear processes affected by small ubiquitin-like modifier conjugation in *Arabidopsis. Proc. Natl. Acad. Sci. U.S.A.* **107,** 16512–16517
42. Tatham, M. H., Matic, I., Mann, M., and Hay, R. T. (2011) Comparative proteomic analysis identifies a role for SUMO in protein quality control. *Sci. Signal* **4,** rs4
43. Li, T., Evdokimov, E., Shen, R. F., Chao, C. C., Tekle, E., Wang, T., Stadtman, E. R., Yang, D. C., and Chock, P. B. (2004) SUMOylation of heterogeneous nuclear ribonucleoproteins, zinc finger proteins, and nuclear pore complex proteins: a proteomic analysis. *Proc. Natl. Acad. Sci. U.S.A.* **101,** 8551–8556
44. Zhou, W., Ryan, J. J., and Zhou, H. (2004) Global analyses of SUMOylated proteins in *Saccharomyces cerevisiae*. Induction of protein SUMOylation by cellular stresses. *J. Biol. Chem.* **279,** 32262–32268
45. Elrouby, N., and Coupland, G. (2010) Proteome-wide screens for small ubiquitin-like modifier (SUMO) substrates identify *Arabidopsis* proteins implicated in diverse biological processes. *Proc. Natl. Acad. Sci. U.S.A.* **107,** 17415–17420
46. Schutz, W., Hausmann, N., Krug, K., Hampp, R., and Macek, B. (2011) Extending SILAC to proteomics of plant cell lines. *Plant Cell* **23,** 1701–1705
47. Schulze, W. X., and Usadel, B. (2010) Quantitation in mass-spectrometry-based proteomics. *Annu. Rev. Plant Biol.* **61,** 491–516
48. Casado-Vela, J., Martinez-Esteso, M. J., Rodriguez, E., Borras, E., Elortza, F., and Bru-Martinez, R. (2010) iTRAQ-based quantitative analysis of protein mixtures with large fold change and dynamic range. *Proteomics* **10,** 343–347
49. Kocher, T., Pichler, P., Schutzbier, M., Stingl, C., Kaul, A., Teucher, N., Hasenfuss, G., Penninger, J. M., and Mechtler, K. (2009) High precision quantitative proteomics using iTRAQ on an LTQ Orbitrap: a new mass spectrometric method combining the benefits of all. *J. Proteome Res.* **8,** 4743–4752
50. Saracco, S. A., Hansson, M., Scalf, M., Walker, J. M., Smith, L. M., and Vierstra, R. D. (2009) Tandem affinity purification and mass spectrometric analysis of ubiquitylated proteins in *Arabidopsis. Plant J.* **59,** 344–358
51. Rohrbough, J. G., Breci, L., Merchant, N., Miller, S., and Haynes, P. A. (2006) Verification of single-peptide protein identifications by the application of complementary database search algorithms. *J. Biomol. Tech.* **17,** 327–332
52. Ow, S. Y., Salim, M., Noirel, J., Evans, C., Rehman, I., and Wright, P. C. (2009) iTRAQ underestimation in simple and complex mixtures: "the good, the bad and the ugly." *J. Proteome Res.* **8,** 5347–5355
53. Ren, J., Gao, X., Jin, C., Zhu, M., Wang, X., Shaw, A., Wen, L., Yao, X., and Xue, Y. (2009) Systematic study of protein SUMOylation: development of a site-specific predictor of SUMOsp 2.0. *Proteomics* **9,** 3409–3412

54. Wenger, C. D., Lee, M. V., Hebert, A. S., McAlister, G. C., Phanstiel, D. H., Westphall, M. S., and Coon, J. J. (2011) Gas-phase purification enables accurate, multiplexed proteome quantification with isobaric tagging. *Nat. Methods* **8,** 933–935
55. Charng, Y. Y., Liu, H. C., Liu, N. Y., Chi, W. T., Wang, C. N., Chang, S. H., and Wang, T. T. (2007) A heat-inducible transcription factor, HsfA2, is required for extension of acquired thermotolerance in *Arabidopsis. Plant Physiol.* **143,** 251–262
56. Rosendorff, A., Sakakibara, S., Lu, S., Kieff, E., Xuan, Y., DiBacco, A., Shi, Y., and Gill, G. (2006) NXP-2 association with SUMO2 depends on lysines required for transcriptional repression. *Proc. Natl. Acad. Sci. U.S.A.* **103,** 5308–5313
57. Moissiard, G., Cokus, S. J., Cary, J., Feng, S., Billi, A. C., Stroud, H., Husmann, D., Zhan, Y., Lajoie, B. R., McCord, R. P., Hale, C. J., Feng, W., Michaels, S. D., Frand, A. R., Pellegrini, M., Dekker, J., Kim, J. K., and Jacobsen, S. (2012) MORC family ATPases required for heterochromatin condensation and gene silencing. *Science* **336,** 1448–1451
58. Panse, V. G., Hardeland, U., Werner, T., Kuster, B., and Hurt, E. (2004) A proteome-wide approach identifies SUMOylated substrate proteins in yeast. *J. Biol. Chem.* **279,** 41346–41351
59. Yang, W., Thompson, J. W., Wang, Z., Wang, L., Sheng, H., Foster, M. W., Moseley, M. A., and Paschen, W. (2012) Analysis of oxygen/glucose-deprivation-induced changes in SUMO3 conjugation using SILAC-based quantitative proteomics. *J. Proteome Res.* **11,** 1108–1117
60. Ferguson, D., Guikema, J., and Paulsen, G. (1989) Ubiquitin pool modulation and protein degradation in wheat roots during high temperature stress. *Plant Physiol.* **92,** 740–746
61. Bossis, G., and Melchior, F. (2006) Regulation of SUMOylation by reversible oxidation of SUMO conjugating enzymes. *Mol. Cell* **21,** 349–357
62. Sydorskyy, Y., Srikumar, T., Jeram, S. M., Wheaton, S., Vizeacoumar, F. J., Makhnevych, T., Chong, Y. T., Gingras, A. C., and Raught, B. (2010) A novel mechanism for SUMO system control: regulated Ulp1 nucleolar sequestration. *Mol. Cell. Biol.* **30,** 4452–4462
63. Davletova, S., Rizhsky, L., Liang, H., Shengqiang, Z., Oliver, D. J., Coutu, J., Shulaev, V., Schlauch, K., and Mittler, R. (2005) Cytosolic ascorbate peroxidase 1 is a central component of the reactive oxygen gene network of *Arabidopsis. Plant Cell* **17,** 268–281
64. Blomster, H. A., Hietakangas, V., Wu, J., Kouvonen, P., Hautaniemi, S., and Sistonen, L. (2009) Novel proteomics strategy brings insight into the prevalence of SUMO-2 target sites. *Mol. Cell. Proteomics* **8,** 1382–1390
65. Meier, I. (2012) mRNA export and SUMOylation—lessons from plants. *Biochim. Biophys. Acta* **1819,** 531–537
66. Lyst, M. J., and Stancheva, I. (2007) A role for SUMO modification in transcriptional repression and activation. *Biochem. Soc. Trans.* **35,** 1389–1392
67. Rosonina, E., Duncan, S. M., and Manley, J. L. (2010) SUMO functions in constitutive transcription and during activation of inducible genes in yeast. *Genes Dev.* **24,** 1242–1252
68. Ausin, I., Mockler, T. C., Chory, J., and Jacobsen, S. E. (2009) IDN1 and IDN2 are required for *de novo* DNA methylation in *Arabidopsis thaliana. Nat. Struct. Mol. Biol.* **16,** 1325–1327
69. Muthuswamy, S., and Meier, I. (2011) Genetic and environmental changes in SUMO homeostasis lead to nuclear mRNA retention in plants. *Planta* **233,** 201–208
70. Xu, X. M., Rose, A., Muthuswamy, S., Jeong, S. Y., Venkatakrishnan, S., Zhao, Q., and Meier, I. (2007) NUCLEAR PORE ANCHOR, the *Arabidopsis* homolog of Tpr/Mlp1/Mlp2/megator, is involved in mRNA export and SUMO homeostasis and affects diverse aspects of plant development. *Plant Cell* **19,** 1537–1548
71. Goodson, M. L., Hong, Y., Rogers, R., Matunis, M. J., Park-Sarge, O. K., and Sarge, K. D. (2001) SUMO-1 modification regulates the DNA binding activity of heat shock transcription factor 2, a promyelocytic leukemia nuclear body associated transcription factor. *J. Biol. Chem.* **276,** 18513–18518
72. Hong, Y., Rogers, R., Matunis, M. J., Mayhew, C. N., Goodson, M. L., Park-Sarge, O. K., Sarge, K. D., and Goodson, M. (2001) Regulation of heat shock transcription factor 1 by stress-induced SUMO-1 modification. *J. Biol. Chem.* **276,** 40263–40267
73. Anckar, J., Hietakangas, V., Denessiouk, K., Thiele, D. J., Johnson, M. S., and Sistonen, L. (2006) Inhibition of DNA binding by differential SUMOylation of heat shock factors. *Mol. Cell. Biol.* **26,** 955–964
74. Xie, Y., Kerscher, O., Kroetz, M. B., McConchie, H. F., Sung, P., and Hochstrasser, M. (2007) The yeast Hex3/Slx8 heterodimer is a ubiquitin ligase stimulated by substrate SUMOylation. *J. Biol. Chem.* **282,** 34176–34184
75. Sun, H., Leverson, J. D., and Hunter, T. (2007) Conserved function of RNF4 family proteins in eukaryotes: targeting a ubiquitin ligase to SUMOylated proteins. *EMBO J.* **26,** 4102–4112
76. Hua, Z., and Vierstra, R. D. (2011) The cullin-RING ubiquitin-protein ligases. *Ann. Rev. Plant Biol.* **62,** 299–334